JACS
JOURNAL OF THE AMERICAN CHEMICAL SOCIETY
Article
pubs.acs.org/JACS

High-Performance Graphene Oxide Electromechanical Actuators

Geoffrey W. Rogers* and Jefferson Z. Liu*

Department of Mechanical and Aerospace Engineering, Monash University, Clayton, Victoria 3800, Australia

Supporting Information

ABSTRACT: Having demonstrated unparalleled actuation stresses and strains, covalently bonded carbon-based nanomaterials are emerging as the actuators of the future. To exploit their full potential, further investigations into the optimum configurations of these new materials are essential. Using first-principle density functional calculations, we examine so-called clamped and unzipped graphene oxide (GO) as potential electromechanical actuator materials. Very high strains are predicted for hole injection into GO, with reversible and irreversible values of up to 6.3% and 28.2%, respectively. The huge 28% irreversible strain is shown to be the result of a change in the atomic structure of GO from a metastable clamped to more stable unzipped configuration. Significantly, this strain generation mechanism makes it possible to hold a constant strain of 23.8% upon removal of the input power, making this material ideal for long-term, low-power switching applications. A unique contraction of unzipped GO upon electron injection is also observed. It is shown that the origin of this unique behavior is the modulation of the structural rippling effect, which is a characteristic feature of GO. With reversible strains and stresses in excess of 5% and 100 GPa, respectively, GO is poised to be an extremely useful material for micro/nanoelectromechanical system actuators.

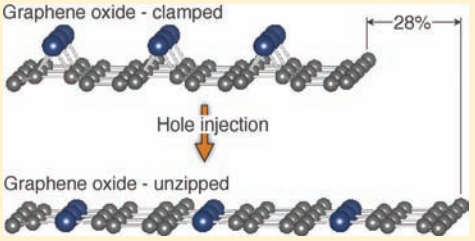

INTRODUCTION

Since the first demonstration of a carbon nanotube (CNT) actuator in 1999,[1] the actuation of covalently bonded carbon-based nanomaterials has attracted much interest.[2−8] This is not surprising given that these materials have already been shown capable of generating both higher stresses than natural muscle and higher strains than high-modulus ferroelectric materials.[1] In addition, these materials possess other inherent strengths, including the ability to operate under extreme temperature conditions.[1,9] To realize the full potential of these materials for micro/nanoelectromechanical system (MEMS/NEMS) applications, further investigation is required to understand the origin of, and to optimize, their actuation performances. In a recent study, we investigated the physics behind the actuation of pristine monolayer graphene, where it was shown that quantum-mechanical strains of 0.2% are expected for charge injections of −0.1 e/C atom.[8] While these strains exceed those produced by widely used high-modulus ferroelectric materials (∼0.1%), it may be possible to extract further actuation performance from graphene-based nanomaterials.

The chemical exfoliation of bulk graphite has become a popular method of synthesizing graphene, due to its potential for economical large-scale production.[10] This process involves the oxidation and reduction of crystalline graphite, which leads to the synthesis of graphene oxide (GO)[11] as a prereduction product.[10,12] Due to this ease of bulk manufacture, and thus its availability, GO has generated wide applicational interest, including for thermomechanical actuation.[13] Studies investigating GO have found that different atomic structures are attainable, which give rise to differing electronic and mechanical properties.[14−19] In a recent experimental investigation, local GO periodic structures, representative of the highly ordered doping of single oxygen (O) atoms onto the hexagonal lattice of pristine graphene, were observed.[15] Interestingly, approximately 50% of the GO surfaces characterized in this study were found to comprise these novel periodic structures, within which two distinct O atom doping configurations are believed to exist: so-called clamped and unzipped. In the clamped case, the in-plane lattice constant of the doped graphene was found to be very similar to that of pristine graphene. For this to be possible, it is believed that each dopant O atom binds to two C atoms in the graphene lattice, without rupturing the adjoining C−C bond (see Figure 1a).[15,16] For the unzipped case, the in-plane lattice constant was much greater than that of pristine graphene, indicating that the C−C bond is ruptured, unzipping the lattice into conjoined graphene nanoribbons (see Figure 1b).[15,16] An interesting feature of GO (clamped and unzipped) is that it exhibits a unique structural phenomenon, herein referred to as rippling. As shown in Figure 1, this prevents the GO lattice from lying completely flat, in contrast to pristine graphene, which relaxes into a nearly perfect 2D plane.[16,18,20] The extent of the rippling differs considerably between the clamped and unzipped configurations of GO. We note that the rippling of GO is a short-range periodic effect (∼10 Å), in contrast to the longer range perturbations that are observed in stable monolayer graphene sheets.[21]

Given the significant difference in atomic structure between clamped and unzipped GO, it is foreseeable that each could behave very differently upon electromechanical actuation. Using first-principle density functional calculations, in this study we seek to investigate this concept in-depth and to

Received: October 12, 2011
Published: December 8, 2011

dx.doi.org/10.1021/ja2096199 | J. Am. Chem.Soc. 2012, 134, 1250−1255

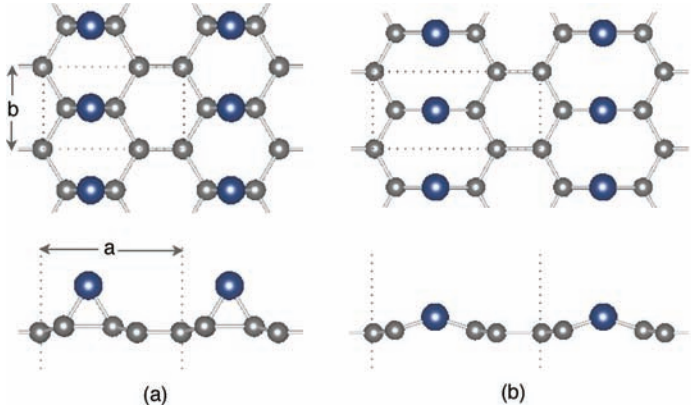

In-plane lattice parameters (Å)

	a	b
Clamped	4.332	2.545
Unzipped	5.359	2.476
Graphene	4.268	2.464

Figure 1. Symmetrically clamped (a) and unzipped (b) GO configurations. In each case the C_4O unit cells are depicted by dotted lines, with the corresponding in-plane lattice parameters shown inset (along with those of pristine graphene). The C and O atoms are represented by small silver and large blue spheres, respectively.

establish the potential for exploitation of GO as an MEMS/NEMS actuator material. If it is possible to modulate the degree of rippling in the respective GO structures, this effect could serve as an origin for a new graphene-based in-plane actuation mechanism. Additionally, constructive addition of this rippling strain and the quantum-mechanical interatomic bond length strain could yield significantly better performances than previously observed and predicted for covalently bonded carbon materials.

COMPUTATIONAL METHOD

Density functional computations of the clamped and unzipped GO materials were performed using the Vienna Ab-initio Simulation Package (VASP, version 5.2.2). Projector augmented wave (PAW) pseudopotentials and the generalized gradient approximation (GGA) were used,[22,23] with a plane-wave cutoff energy of 400 eV. Figure 1 shows the clamped and unzipped unit cells used to model GO in this study (for atomic coordinates, see the Supporting Information, Figure S1 and Table S1). Our investigation focuses on the novel periodic GO configurations that have been observed by others,[15] as these more orderly structures, compared to nonstoichiometric GO, could provide the ability to accurately fine-tune an actuator's properties to suit a given application. For comparison, pristine monolayer graphene was also simulated using the same C_4 cell geometry as for the case of GO, albeit in the absence of the O atoms. All structures were fully relaxed to their respective ground states prior to charge injection. A Monkhorst–Pack γ-centered k-point grid of dimensions $24 \times 42 \times 1$ was adopted for the clamped GO and pristine graphene cells, with a $20 \times 42 \times 1$ grid for the unzipped GO cell.

Injected charges (electrons and holes) were compensated using a background jellium to maintain charge neutrality in the unit cell. As VASP employs periodic boundary conditions, very thick vacuum layers were included adjacent to the GO sheets to minimize interlayer electrostatic interactions. As shown previously, this minimizes the jellium self-energy contribution to the overall strain, and thus realistically predicts the true quantum-mechanical actuation.[8] An interlayer spacing of 60 Å was used throughout, which provided a good balance between computational accuracy and effort.[8] To hold this interlayer spacing constant, the VASP source code was modified to allow the cell to completely relax within the plane of the GO and graphene layers only, not perpendicular to the plane. In all cases, all C and O ions comprising the respective cells were allowed to relax freely in all directions.

RESULTS AND DISCUSSION

The in-plane strains, measured as the change in lattice parameter a, for charge injection into both GO configurations (Figure 1) and pristine monolayer graphene are shown in Figure 2. The most pronounced feature is that very high strains

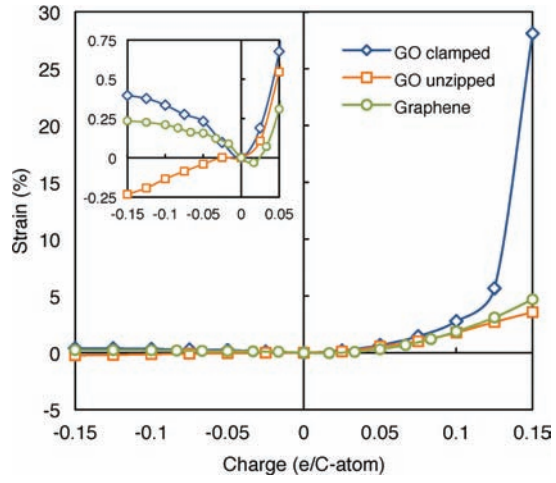

Figure 2. Actuation of GO (clamped and unzipped) and pristine graphene due to positive (hole) and negative (electron) charge injection. Inset: close-up of the strain responses between −0.15 and +0.05 e/C atom charge injection.

are observed for hole (positive charge) injection into GO, especially for the clamped configuration, where a hole injection of 0.15 e/C atom induces a massive 28.2% strain. While others have demonstrated intertube electrostatic strains in excess of 10% for strips of aligned CNT sheets,[2] the significance of the present 28.2% strain is that it acts along a covalently bonded axis of the material. From Figure 2 it is evident that the same hole injection into unzipped GO and pristine graphene produces strains of 3.6% and 4.7%, respectively, which are significantly less than the clamped GO prediction of 28.2%. The exact origin of this immense actuation performance is addressed later in this paper.

Further inspection of Figure 2 (inset) reveals that electron injection into clamped GO produces a charge–strain relationship very similar to that of pristine graphene, exhibiting expansions of up to 0.4% for a −0.15 e/C atom charge. Conversely, the charge–strain dependency of unzipped GO is distinctly dissimilar to those of clamped GO and pristine graphene, contracting upon electron injection. This is contrary to what is expected for the quantum-mechanical actuation of

dx.doi.org/10.1021/ja2096199 | J. Am. Chem.Soc. 2012, 134, 1250–1255

covalent carbon materials, such as graphene and CNTs, where injected electrons are believed to fill antibonding states and thus induce interatomic bond length expansions.[7,24] To explain this peculiar observation, recall that GO has a unique structural property, referred to as rippling, which we hypothesized could give rise to interesting actuation behavior. As this rippling effect is an out-of-plane structural phenomenon, it is possible for the unzipped GO structure to undergo an interatomic bond length expansion, while the unit cell experiences a net contraction along the *a* axis. To investigate, Figure 3 shows the expansion

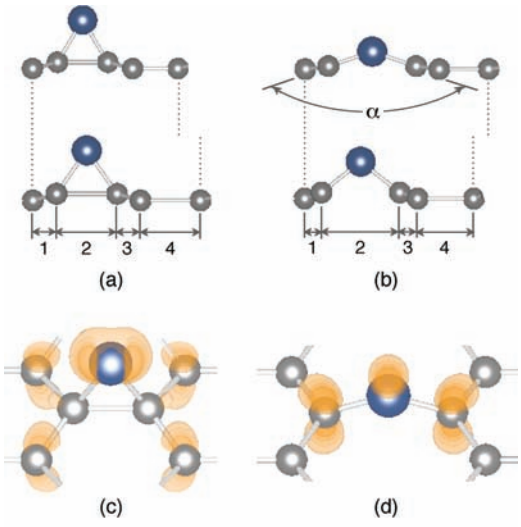

***a*-axis deformations (Å)**

	Clamped	Unzipped
1	−0.0016	−0.0050
2	0.0082	−0.0085
3	−0.0016	−0.0050
4	0.0122	0.0061
Total	0.0172	−0.0124

Figure 3. Total strain response of clamped (a) and unzipped (b) GO upon electron injection. Unlike the clamped case, unzipped GO contracts upon electron injection due to structural rippling modulation, which can be quantified by the C−O−C bond angle α. In each case the deformed cell is contrasted with the undeformed cell directly above. The excess charge density profiles for clamped (c) and unzipped (d) GO explain the observed actuation behavior upon electron injection (orange regions represent excess electron density). Inset: *a* axis resolved interatomic deformations, where the numbers correspond to the respective positions indicated in (a) and (b). The profiles and deformations shown are for a −0.15 e/C atom charge injection.

and contraction of clamped (Figure 3a) and unzipped (Figure 3b) GO, respectively, for a −0.15 e/C atom charge injection. In Figure 3a, the interatomic bonds of clamped GO expand upon electron injection, while the rippling within the structure remains unchanged, leading to an expansion of the unit cell along the *a* axis. This effect is identical to the actuation of pristine graphene upon electron injection in the absence of structural rippling. In Figure 3b, the interatomic bond lengths of unzipped GO also change, but this time the extent of the structural rippling also changes. We have quantified the extent of the rippling by the C−O−C bond angle α as indicated, which remains constant during pure interatomic bond length expansion/contraction. For the unzipped case, an increase in the structural rippling effect, and thus a decrease in the C−O−C bond angle α, leads to a contraction of the unit cell along the *a* axis.

To verify this proposed unzipped GO contraction origin, which is quantum-mechanical in nature, it is necessary to consider and compare the clamped (Figure 3c) and unzipped (Figure 3d) excess charge density distributions.[25] For the unzipped case (Figure 3d), the −0.15 e/C atom injected charge aggregates atop the O atom and also atop and beneath the O-bonded C atoms. It is evident that the excess charge on the C atoms is repelled by that on the O atom, as the charge contours lean away from the O atom. This repulsive force between the bonded O and C atoms results in a torque about the O atom, which causes the bond angle α to decrease and the rippling to increase. This is contrasted with the clamped case (Figure 3c), where the excess injected charge aggregates aside the O atom and atop and beneath the *non*-O-bonded C atoms. This time, the excess charge contours indicate that there is a repulsive force acting between the two non-O-bonded C atoms, which leads to an expansion of their C−C bond.

To further validate this, the table in Figure 3 reports the measured *a* axis resolved individual-bond and total deformations. The most significant difference between the clamped and unzipped GO deformations occurs for dimension 2. Here, clamped GO experiences a significant expansion (0.0082 Å), while unzipped GO exhibits a significant contraction (−0.0085 Å). Another interesting observation for clamped and unzipped GO is that dimensions 1 and 3 contract for both configurations, but by varying amounts. For clamped GO the contraction is small (−0.0016 Å), but is more significant for unzipped GO (−0.005 Å). In both cases, the contraction of dimensions 1 and 3 is due to an increase in the C−C−C bond angle of the C ring, in response to the repulsive forces between the non-O-bonded C atoms (Figure 3c). Also worth noting is that both the clamped and unzipped configurations experience an expansion of dimension 4. The aforementioned large repulsive force between the non-O-bonded C atoms for the clamped case gives rise to a large expansion (0.0122 Å), while the relatively smaller excess charge density located at the non-O-bonded C atoms for the unzipped case causes a smaller expansion (0.0061 Å).[26]

To quantify the extent of the rippling modulation contribution to the overall strain, Figure 4 depicts the breakdown of this and the interatomic bond length changes. Here, the interatomic bond length contribution was calculated by summing the individual interatomic bond length changes along the *a* axis for a single unit cell, leading to a prediction of the strain that would be measured if the GO sheet was effectively flat (unrippled). It was then possible to isolate the rippling modulation strains by subtracting the interatomic bond length strains from the total strains of Figure 2. First, from Figure 4a it is strikingly apparent that the rippling modulation effect contributes very little to the total strain for the clamped GO case, with the interatomic bond length and total strains exhibiting a very close relationship across the entire charge injection window. Recall from Figure 2 that clamped GO behaved very similarly to pristine graphene, which agrees with this result. We expect that rippling modulation in clamped GO is not significant because of the C−C bond presence beneath the doped O atoms, which results in the clamped GO structure

dx.doi.org/10.1021/ja2096199 | *J. Am. Chem.Soc.* 2012, 134, 1250−1255

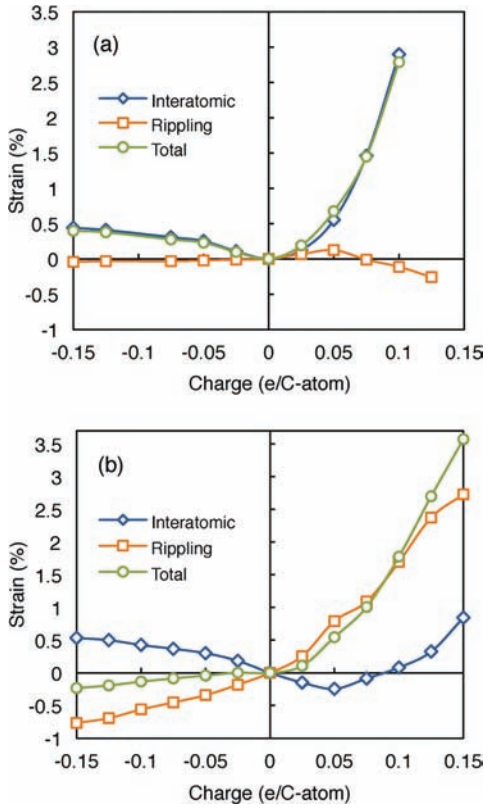

Figure 4. Total, interatomic and rippling strains of clamped (a) and unzipped (b) GO as a function of charge injection. The extents of the contribution by each effect to the total clamped and unzipped GO responses are distinctly different.

retaining the predominant mechanical characteristics of the pristine graphene lattice. In contrast, for the case of unzipped GO (Figure 4b), rippling modulation has a significant effect on the total strain. Interestingly, the interatomic bond length charge–strain relationship in this case is very similar to that of pristine graphene, even displaying the same initial contraction for low hole injection levels (see the pristine graphene case in Figure 2). Despite the similarity between the interatomic bond length and pristine graphene strains, the total unzipped GO charge–strain relationship is far more representative of the rippling modulation strain, at all times having the same strain sign (expansion/contraction). This is also supported by an observed strong positive correlation between the total strain response of unzipped GO and the change in structural rippling, as defined by changes in the C–O–C bond angle (see the Supporting Information, Figure S2). This demonstrates that it is possible to generate unique and high strain responses via modulation of the structural rippling for unzipped GO.

To explain the huge 28.2% strain performance of clamped GO, Figure 5 shows the energy configuration of C_4O GO as a function of the lattice parameter a and the extent of hole injection. As presented and discussed by Xu and Xue,[16] the clamped structure represents a so-called metastable phase of GO, while the unzipped case is the more stable one. Despite the higher stability of the unzipped configuration, it is nonetheless possible to synthesize clamped GO for use in practical MEMS/NEMS actuators,[15] due to the relatively high energy barrier (0.63 eV per unit cell) that separates these two states. To understand the origin of the measured 28.2% strain, consider the 0.63 eV per unit cell energy barrier between the

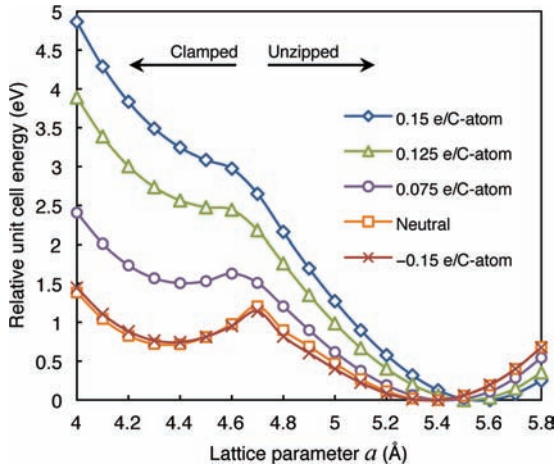

Figure 5. Relative total energy of the GO unit cell as a function of the in-plane lattice parameter a and injected charge. The regions corresponding to the metastable clamped and more stable unzipped configurations are as indicated.

clamped and unzipped phases (between a values of 4.33 and 4.7 Å in Figure 5). Upon hole injection into clamped GO, the energy profile is modified (Figure 5), which results in an expansion of the unit cell along the a axis (see also Figure 2). This expansion is due to the concentration of excess holes on the O atom, as well as at and between the O-bonded C atom sites, which weakens the adjoining C–C bond (Figure 6). With

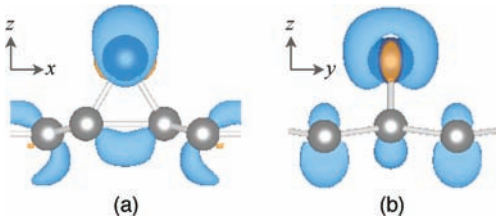

Figure 6. The excess charge density profile of clamped GO upon 0.15 e/C atom hole injection explains the observed expansion and eventual unzipping of GO (blue (orange) regions represent excess hole (electron) densities): (a) view along the zigzag (y) direction; (b) view along the armchair (x) direction.

further hole injection, the energy profile continues to change until the energy barrier between the clamped and unzipped configurations disappears, and the clamped unit cell *snaps* from an initial lattice constant of 4.33 to 5.55 Å (while charged). This is the point at which the bond between the O-bonded C atoms is weakened to such an extent that it ruptures, which is the configurational origin of the predicted 28.2% strain. An interesting feature of this actuation mechanism is that it is possible to actuate the material by 28.2% and then remove the input power without the strain returning to zero (a will relax to 5.36 Å upon charge removal, which corresponds to a 23.8% strain). This is since the material will maintain its new unzipped configuration once the C–C bonds beneath the O atoms have ruptured and the new C–O–C bonds have formed. This feature would be particularly beneficial for long-term, low-power switching applications.

Practically speaking, it is typically desirable that induced actuation be fully reversible. Due to the very high energy barrier on the approach side from the unzipped to clamped configurations in Figure 5 (1.33 eV between a values of 4.7

dx.doi.org/10.1021/ja2096199 | J. Am. Chem.Soc. 2012, 134, 1250–1255

and 5.36 Å), it would seem difficult to reverse the 28.2% strain. To do so would require an increase in the extent of the unzipped GO rippling and thus a decrease in the C−O−C bond angle α, which can only be achieved via the injection of electrons as discussed earlier (see also Supporting Information, Figure S2). From Figure 5, the lattice parameter a would need to be decreased from 5.36 to 4.75 Å, about −11.4%. It is evident that even the maximum electron injection level (−0.15 e/C atom) has little effect on the overall energy profile (Figure 5), which agrees with the results of Figure 2 (a strain of only −0.23% is attainable for −0.15 e/C atom electron injection). Hence, reversal of the 28.2% strain would require some additional influence to charge injection alone. Nonetheless, if only irreversible actuation of GO by 28% were possible, this would still be extremely useful for select applications, such as legislated single-use industrial safety switches. In addition, GO can be used for the generation of high reversible strains in a more traditional actuation sense, with clamped GO being capable of generating peak strains of up to 6.3% prior to surpassing the energy barrier and unzipped GO being capable of both large contraction (−0.25%) and expansion (3.6%).

The applicational significance of GO for use in practical actuators is further enhanced by its ability to generate very high stresses (in excess of 100 GPa), due to the characteristic high modulus of pristine monolayer graphene (∼1 TPa)[27] and GO (∼0.6 TPa)[16] along covalently bonded directions (for GO and pristine graphene actuation stresses, see the Supporting Information, Figure S3). By way of comparison with other actuation materials, the volumetric work density of GO for a 0.125 e/C atom charge injection, which equates to the highest reversible strain of 6.3%, is 52.9 J/cm^3 (based on the computed strain energy). This is approximately double the value reported for the first CNT-based actuation material,[1] and about 53 times greater than the highest values presented for the widely used ferroelectric materials.[28] We also calculated the work density of pristine monolayer graphene for the highest strain predicted herein (4.7%), which we found to be 54.1 J/cm^3. This value is slightly greater than that of GO, due to the small difference in the respective moduli. Another important practical consideration is the voltage required to inject the herein reported charges into graphene and GO.[29] On the basis of Fermi-level shift measurements from the integrated density of states (DOS) upon charge injection,[30] we estimate the voltages required to inject 0.15 e/C atom charges (both electrons and holes) into graphene and GO to be 2−4 V. An additionally important consideration is that monolayer materials have very low out-of-plane structural integrities and so are prone to buckling upon loading. While the aim of this work was to investigate the electromechanical response of GO at the ultimate limit (a single layer), it is foreseeable that monolayer GO actuators could be used in MEMS/NEMS devices by coupling a GO layer with one or more pristine graphene layers (a substrate), for example. Because the GO and graphene layers would only be held together by weak van der Waals interactions and GO generates very high in-plane forces, the GO would be able to slide along the graphene substrate upon actuation. All of this suggests that GO is a very attractive material for high-performance actuator applications. Noting that these results are for the ultimate limit of GO (a single layer) and that many MEMS/NEMS applications will require larger actuator volumes, we expect that our findings will be applicable to, and guide the design of, few/many layer GO electromechanical actuators.

While this investigation focuses on the more recently observed periodic GO configurations, containing epoxy groups only, we note that other GO configurations may also contain basal plane hydroxyl groups (e.g., the Lerf−Klinowski model[31]). Such groups can be included in our model to extend our investigations to these cases. To ascertain the effect that hydroxyl groups could have on our results, and thus the transferability of our findings, we conducted preliminary investigations by adding these groups to our model in accordance with the models established by recently published findings.[17−20] Initial results suggest that the inclusion of hydroxyl groups within our C_4 unit cells has only a minor effect on the reported electromechanical stresses and strains. As such, we expect our conclusions to be transferable to these other GO structures. A separate structural consideration is that the herein actuation mechanism is based on the short-range structural rippling of GO, for which basal plane alignment of the epoxy groups is necessary. This represents a scenario distinctly different from that of the nonstoichiometric graphite oxide configurations that have long been investigated. Many researchers have established that epoxy groups are more stable than hydroxyl groups in terms of their basal plane binding energies and further that epoxy groups energetically prefer to align than distribute randomly.[16−20] Such alignment has also been observed in experiments[14,15] where the GO was prepared via the Hummers method.[32] The fact that approximately 50% of these Hummers-synthesized GO sheets comprised highly aligned epoxy-only structures,[15] where there is an abundance of hydrogen (H) present to react with the graphene and form hydroxyl groups, confirms the thermodynamic stability of these configurations. However, to more reliably produce larger areas (>50%) of this highly ordered GO, it could be advantageous to instead prepare the GO by oxidizing mechanically exfoliated flakes in a humidity-controlled ultrahigh vacuum (UHV) to further restrict H adsorption and hydroxyl formation.

CONCLUSIONS

The electromechanical actuation of two distinct configurations of GO (clamped and unzipped) was studied using first-principle density functional calculations. Two very significant features of the GO actuation response were highlighted and explained. The first was the unique contraction of unzipped GO upon electron injection, which was shown to be the result of modulation of the structural rippling effect, an interesting characteristic of GO. The second of these features was the ability of clamped GO to generate strains of up to 28.2%, the origin of which was a change in the atomic structure from the metastable clamped configuration to the more stable unzipped configuration. Hole injection levels sufficient to raise the energy of the clamped GO unit cell above the threshold of the energy barrier separating the two configurations made this possible. The potential use of GO as an MEMS/NEMS actuator material, such as for artificial muscle applications, is very pronounced. With reversible strains ranging between −0.25% and +6.3% and massive irreversible strains of up to 28.2%, the electromechanical performance of this material is far superior to that of pristine graphene. Additionally, with its very high stress capacities (>100 GPa), GO could pave the way for previously unachievable actuator applications requiring very high stress and strain generation.

dx.doi.org/10.1021/ja2096199 | J. Am. Chem.Soc. 2012, 134, 1250−1255

■ ASSOCIATED CONTENT

Supporting Information

A figure and table giving the coordinates of all atoms comprising the unit cells of GO (clamped and unzipped) and pristine graphene, a figure showing the structural rippling−total strain correlation for unzipped GO, and a figure showing the actuation stresses of GO and pristine graphene as a function of charge injection. This material is available free of charge via the Internet at http://pubs.acs.org.

■ AUTHOR INFORMATION

Corresponding Author

geoff.rogers@monash.edu; zhe.liu@monash.edu

■ ACKNOWLEDGMENTS

We thank the Victorian Partnership for Advanced Computing for their support of this research. This work was also supported by an award under the Merit Allocation Scheme of the National Computational Infrastructure (NCI) facility at the Australian National University. J.Z.L. acknowledges the support of the Faculty of Engineering, Monash University (Small Grant).

■ REFERENCES

(1) Baughman, R.; Cui, C.; Zakhidov, A.; Iqbal, Z.; Barisci, J.; Spinks, G.; Wallace, G.; Mazzoldi, A.; DeRossi, D.; Rinzler, A.; Jaschinski, O.; Roth, S.; Kertesz, M. *Science* **1999**, *284*, 1340.

(2) Aliev, A.; Oh, J.; Kozlov, M.; Kuznetsov, A.; Fang, S.; Fonseca, A.; Ovalle, R.; Lima, M.; Haque, M.; Gartstein, Y.; Zhang, M.; Zakhidov, A.; Baughman, R. *Science* **2009**, *323*, 1575.

(3) Xie, X.; Qu, L.; Zhou, C.; Li, Y.; Zhu, J.; Bai, H.; Shi, G.; Dai, L. *ACS Nano* **2010**, *4*, 6050.

(4) Hughes, M.; Spinks, G. *Adv. Mater.* **2005**, *17*, 443.

(5) Suppiger, D.; Busato, S.; Ermanni, P. *Carbon* **2008**, *46*, 1085.

(6) Sun, G.; Kürti, J.; Kertesz, M.; Baughman, R. *J. Am. Chem. Soc.* **2002**, *124*, 15076.

(7) Verissimo-Alves, M.; Koiller, B.; Chacham, H.; Capaz, R. *Phys. Rev. B* **2003**, *67*, 161401.

(8) Rogers, G.; Liu, J. Z. *J. Am. Chem. Soc.* **2011**, *133*, 10858.

(9) Choi, W.; Abrahamson, J.; Strano, J.; Strano, M. *Mater. Today* **2010**, *13*, 22.

(10) Tung, V.; Allen, M.; Yang, Y.; Kaner, R. *Nat. Nanotechnol.* **2008**, *4*, 25.

(11) The acronym GO sometimes refers to bulk *graphite* oxide. Here we use it to refer to monolayer *graphene* oxide.

(12) Eda, G.; Fanchini, G.; Chhowalla, M. *Nat. Nanotechnol.* **2008**, *3*, 270.

(13) Oh, J.; Kozlov, M.; Carretero-González, J.; Castillo-Martínez, E.; Baughman, R. *Chem. Phys. Lett.* **2011**, *505*, 31.

(14) Li, J. L.; Kudin, K.; McAllister, M.; Prud'homme, R.; Aksay, I.; Car, R. *Phys. Rev. Lett.* **2006**, *96*, 176101.

(15) Pandey, D.; Reifenberger, R.; Piner, R. *Surf. Sci.* **2008**, *602*, 1607.

(16) Xu, Z.; Xue, K. *Nanotechnology* **2010**, *21*, 045704.

(17) Yan, J.; Xian, L.; Chou, M. *Phys. Rev. Lett.* **2009**, *103*, 086802.

(18) Boukhvalov, D.; Katsnelson, M. *J. Am. Chem. Soc.* **2008**, *130*, 10697.

(19) Kawai, T.; Miyamoto, Y. *Curr. Appl. Phys.* **2011**, *11*, S50.

(20) Xiang, J.; Wei, S.; Gong, X. *Phys. Rev. B* **2010**, *82*, 035416.

(21) Xu, Z.; Buehler, M. *ACS Nano* **2010**, *4*, 3869.

(22) Kresse, G.; Furthmüller, J. *Phys. Rev. B* **1996**, *54*, 169.

(23) Kresse, G.; Joubert, D. *Phys. Rev. B* **1999**, *59*, 1758.

(24) Kertesz, M.; Vonderviszt, F.; Hoffman, R. *Mater. Res. Symp. Proc.* **1983**, *20*, 141.

(25) Excess charge densities were calculated by taking the difference between the fully relaxed charged and neutral charge densities output by VASP. Neutral charge densities were computed using the same ionic positions as the charged state.

(26) Small excess charge densities are not visible in this figure, as they fall below the minimum threshold values.

(27) Lee, C.; Wei, X.; Kysar, J.; Hone, J. *Science* **2008**, *321*, 385.

(28) Zhang, Q.; Bharti, V.; Zhao, X. *Science* **1998**, *280*, 2101.

(29) We note that while many GO configurations are zero band gap semiconductors (like pristine graphene), some configurations (e.g., clamped C_4O) have a small but finite band gap of ∼1.4 eV. It is foreseeable that charge could be injected evenly across such a semiconducting GO layer by pairing it with a layer of pristine graphene or by patterning networks of metallic interconnects among the GO, for example.

(30) Fang, T.; Konar, A.; Xing, H.; Jena, D. *Appl. Phys. Lett.* **2007**, *91*, 092109.

(31) Lerf, A.; He, H.; Forster, M.; Klinowski, J. *J. Phys. Chem. B* **1998**, *102*, 4477.

(32) Hummers, W.; Offeman, R. *J. Am. Chem. Soc.* **1958**, *80*, 1339.